# A three-dimensional numerical assessment on the influences of treated sewage effluent on an adjacent seaweed farm with different discharge operations

Zhang, Xu
Uchiyama, Yusuke
Nakayama, Akihiko

(Citation)
AIP Conference Proceedings,2157(2):020031

(Issue Date)
2019-09-18

(Resource Type)
journal article

(Version)
Version of Record

# A three-dimensional numerical assessment on the influences of treated sewage effluent on an adjacent seaweed farm with different discharge operations

Cite as: AIP Conference Proceedings **2157**, 020031 (2019); https://doi.org/10.1063/1.5126566
Published Online: 18 September 2019

Xu Zhang, Yusuke Uchiyama, and Akihiko Nakayama

# A Three-dimensional Numerical Assessment on the Influences of Treated Sewage Effluent on an Adjacent Seaweed Farm with Different Discharge Operations

Xu Zhang[1], Yusuke Uchiyama[1, a)] and Akihiko Nakayama [2]

[1]*Department of Civil Engineering, Kobe University, Japan*
[2] *Department of Environmental Engineering, Universiti Tunku Abdul Rahman, Malaysia*

[a)]Corresponding author: uchiyama@harbor.kobe-u.ac.jp

**Abstract.** Coastal dispersal of sewage effluent from the Tarumi Sewage Treatment Plant located in Osaka Bay, Japan, was investigated with a quadruple-nested high-resolution ROMS model coupled with a 3-D passive tracer model. The study area is quite famous for seaweed farming in the nation, which has been claimed considerably affected by the effluent from the plant, particularly in fall when the seaweed spores are most vulnerable to contamination that counteracts their favorable growth and productivity. We applied the model to three different discharge scenarios to explore possible optimal operations that could reduce the influences. If the discharged volume rate is simply decreased at ~16.7% relative to the baseline case that represents the actual operation, the effluent accumulating in the farm is reduced at ~25.4% showing a significant nonlinearity. A tracer flux analysis demonstrated that the transient component accounting for fluctuating tides and eddies dominates over the time-averaged linear contribution to the effluent accumulation in the cross-shore effluent transport to the farm. By contrast, in the along-shore direction, the linear component leads to increased influx near the surface at the western transect of the farm, while the transient component is more essential to the overall reduction of the incoming tracer flux to the farm. On the other hand, density adjustment of the effluent for suppressing surfacing of buoyant effluent plume released from the bottom-mounted diffusers does not work well as expected, because pronounced far-field dilution takes over the near-source dilution affected by the density adjustment.

## INTRODUCTION

The Seto Inland Sea (SIS) is the largest estuary in Japan, where complex tidal and estuarine circulations form because of complicated coastline with more than 3000 islands. Osaka Bay is located in its northeastern area, encompassing densely populated Osaka and Kobe areas. Historically, the number of "red tide" has increased significantly due to the nutrient loading, resulting in serious water quality deteriorations that damage the aquaculture and marine ecosystem (e.g., Imai et al., 2006 [1]; Terawaki et al., 2003 [2]). A series of environmental preservation policies and laws have worked adequately in improving the water quality in recent years in the SIS (Tomita et al., 2016 [3]). However, Osaka Bay still suffers from severe water pollution. The Tarumi Sewage Treatment Plant (TSTP) is a major wastewater treatment plant in Osaka Bay, resulting in a possible nutrient source to the adjacent seaweed farm. To reduce possible negative influences of the TSTP on the local aquacultures, the local government, the City of Kobe, has constructed an alternative western outfall (**Figure 1b**; indicated by "W") 500 m away from the original central outfall (**Figure 1b**, "C") in the TSTP.

Our previous study (Uchiyama et al., 2018 [4]; hereafter we call U18) reported that the western outfall successfully decreases the accumulation of the TSTP effluent in the adjacent farm by ~28% on average, while the instantaneous effluent concentration lowers at ~50%. Although the diversion outfall works efficiently to reduce the effluent accumulation in the seaweed farm, the further reduction of the influence of the TSTP is still requested by the

*International Symposium on Green and Sustainable Technology (ISGST2019)*
AIP Conf. Proc. 2157, 020031-1–020031-7; https://doi.org/10.1063/1.5126566
Published by AIP Publishing. 978-0-7354-1902-5/$30.00

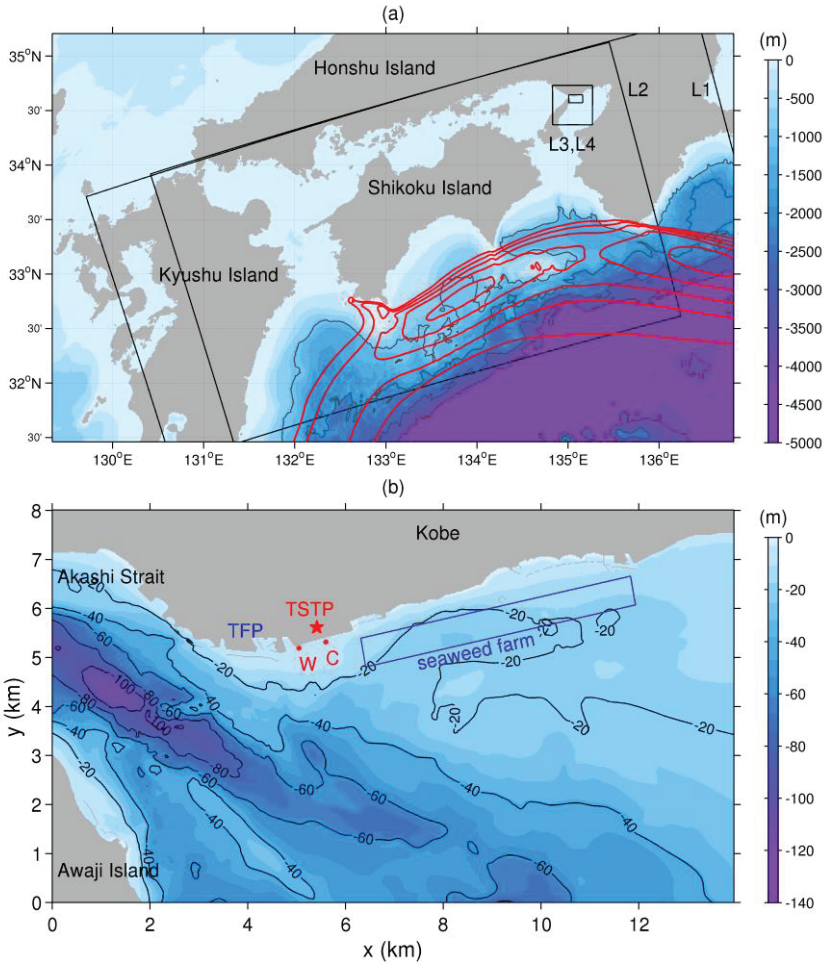


**FIGURE 1.** Quadruple nested ROMS model domains and bathymetry (color: m). (a) The ROMS-L1-L4 (black boxes) embedded in the JCOPE2 domain (outside of the perimeter of the L1). The gray contours are the isobaths with intervals of 1,000 m, while the red contours indicate the approximate Kuroshio region with the surface velocity magnitude greater than 0.5 m $s^{-1}$ at intervals of 0.2 m $s^{-1}$. (b) The L4 domain with isobaths at intervals of 20 m. The red star shows the location of the Tarumi Sewage Treatment Plant (TSTP); the red dots are the two outfalls (W: western alternative outfall, C: central original outfall); the blue box is the approximate seaweed farm area; TFP is the Tarumi Fishery Port area.

local seaweed farmers. Hence, the local government has proposed two possible alternative operations with the diversion outfall 1) by simply decreasing the sewage discharge volume rate, and 2) by increasing the effluent density to diminish its surfacing by mixing with the ambient saline seawater with retaining the nutrient total mass.

In the present study, we used the well-validated JCOPE2-ROMS quadruple-nested model coupled with a 3-D Eulerian passive tracer model to examine the effluent transport of the TSTP in the coastal area with two new discharge operations. The present manuscript mainly concentrated on the influence of the two alternative scenarios on the seaweed farm, and the possible predominant component on the effluent transport.

## THE QUADRUPLE-NESTED JCOPE2-ROMS MODEL

We employed a quadruple-nested downscaling model based on Regional Oceanic Modeling System (ROMS; Shchepetkin and McWilliams, 2005 [5]) model. A 3-D Eulerian passive tracer model (Uchiyama et al., 2014 [6]; U18 [4]) was implemented into the innermost ROMS-L4 model to track the coastal dispersal of the sewage effluent. The

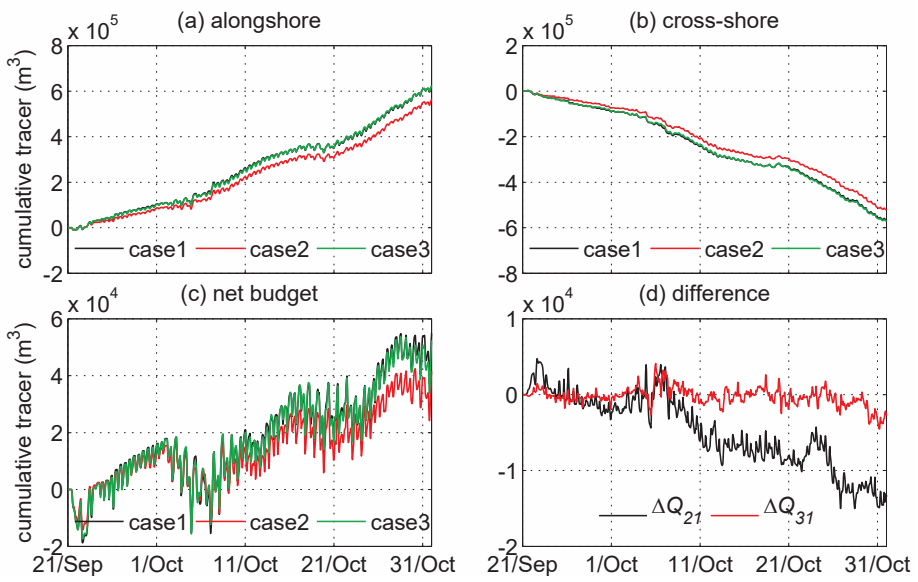


**FIGURE 2**. Time series plot of cumulative tracer fluxes $Q$ ($m^3$) at (a) alongshore and (b) cross-shore directions. (c) Time series plot of net tracer budget accumulating in the seaweed farm. (d) The temporal net tracer budget changes of difference between each case. The blue curve is computed by Case2 – Case1, while the red curve is computed by Case3 – Case1. Note that Case 1 (black curves) varies quite closely with Case 3 in (a)–(c).

assimilative Japan Coastal Ocean Predictability Experiments (JCOPE2) oceanic reanalysis (Miyazawa et al., 2009 [7]) provided the boundary and initial conditions for the outermost ROMS-L1 model. The one-way offline nesting technique (e.g., Mason et al., 2010 [8]; Kamidaira et al., 2017 [9]) was used for downscaling the parent model results into the corresponding child models with grid-size refinement (*i.e.*, JCOPE2 at lateral grid resolution of ~10 km→ L1 at 2 km → L2 at 600 m → L3 at 100 m→ L4 at 20 m). Thus, the innermost ROMS-L4 model resolution ultimately reached 20 m with vertically stretched 32 *s*-layers. The ROMS configurations were the same as those in U18 [4]; for instance, the L4 model was forced by surface wind stress from the Japan Meteorological Agency (JMA) Grid-Point Values–MesoScale Model (GPV-MSM), the monthly climatological surface heat/freshwater fluxes from the Comprehensive Ocean-Atmosphere Data Set (COADS). The principal ten tidal constituents from the TPXO7.0 global reanalysis provided additional sea surface elevation along the open boundaries of the L2 model, which spontaneously generated intrinsic barotropic and baroclinic tides through the open boundaries of the embedded L3 and L4 models. Freshwater discharge from the major rivers was also taken into account whenever needed. The ROMS-L4 model was run for about 50 days to include October of 2015, when the sewage effluent is most influential to the seaweed growth.

## SEWAGE EFFLUENT TRACKING SUBMODEL

The capability of tracking the sewage effluent is implemented into the innermost ROMS-L4 based on the non-dimensional Eulerian passive tracer concentration $c$ with the near-field dilution submodel (Uchiyama et al., 2014 [6]; U18 [4]):

$$\frac{\partial c}{\partial t} + \nabla \cdot \mathbf{u}c = \mathcal{D} + \mathcal{P}, \tag{1}$$

with the non-dimensional source term, $\mathcal{P}$:

$$\mathcal{P}(x, y, z; t) = P_s(t)A(x, y)H(z), \tag{2}$$

where $\mathbf{u}$ is the 3-D velocity of the ambient flow, $\mathcal{D}$ is the diffusion term, $\nabla$ is the 3-D gradient operator, $P_s$ is the tracer flux from the outfall, and $A$ and $H$ are the spatial shape functions of plume above the diffusers. The spatial distributions in the source region are shown in the following integral relations:

**TABLE 1.** Cumulative non-dimensional tracer fluxes in the seaweed farm, $Q_{farm}$ ($m^3$)

| | Until Oct. 3 | Until Oct. 17 | Until Oct. 31 | Average |
|---|---|---|---|---|
| $Q_1$ | $1.84\times10^4$ | $3.67\times10^4$ | $5.49\times10^4$ | $2.01\times10^4$ |
| $Q_2$ | $1.60\times10^4$ | $2.78\times10^4$ | $4.15\times10^4$ | $1.50\times10^4$ |
| $Q_3$ | $1.85\times10^4$ | $3.66\times10^4$ | $5.22\times10^4$ | $1.98\times10^4$ |
| $\Delta Q_{21}$ | $-0.24\times10^4$ | $-0.89\times10^4$ | $-1.34\times10^4$ | $-0.51\times10^4$ |
| $\Delta Q_{31}$ | $0.1\times10^4$ | $-0.01\times10^4$ | $-0.27\times10^4$ | $-0.03\times10^4$ |

Note: $\Delta Q_{21} = Q_2 - Q_1$, $\Delta Q_{31} = Q_3 - Q_1$.

**TABLE 2.** Mean and transient flow components of tracer flux ($m^3$/h)

| | | Case 1 (baseline) | Case 2 | Difference |
|---|---|---|---|---|
| Along-shore direction | $\overline{cu_n}$ | 632.68 | 572.07 | -60.61 |
| | $\bar{c}\,\overline{u_n}$ | -2366.80 | -2018.70 | 348.10 |
| | $\overline{c'u_n'}$ | 2999.48 | 2590.77 | -408.71 |
| Cross-shore direction | $\overline{cu_n}$ | -576.89 | -529.82 | 47.07 |
| | $\bar{c}\,\overline{u_n}$ | 104.16 | 89.44 | -14.72 |
| | $\overline{c'u_n'}$ | -681.05 | -619.26 | 61.79 |

Note: difference: Case 2 – Case1

$$\iint A\,dxdy = A_s, \int H\,dz = H_s, \tag{3}$$

where $A_s$ is the horizontal area, $H_s$ is the vertical size, $V_s = A_s H_s$ is the sewage plume volume. Hence, $P_s(t) = Q_p(t)/V_s$, where $Q_p(t)$ [$m^3\ s^{-1}$] is the volume flux. The dimensional pollutant concentrations are retrieved by multiplying $C_p$, where $C_p$ is the input pollutant concentration at the outfall.

The Gaussian shape function was used for $H$ based on the following equation

$$H(z) = \exp\left[-\frac{(z-z_s)^2}{d_s^2}\right], \tag{4}$$

where $z_s$ is the plume center height, and $d_s$ is the vertical scale of the plume. Because the local depth of 7 m is shallower than the mixed layer, we defined $z_s$ = 0 m and $d_s$ = 7 m in our model. The outfall is set by two grid points (*viz*., a footprint of 20 m × 40 m), where $A$ = 0.5, centered at 40 m offshore from the sea wall of the TSTP, corresponding approximately to the actual diversion outfall length.

The sewage effluent (tracer) is discharged as a bottom-released freshwater plume at the volume rate of $Q_p$ with the prescribed concentration of $c = c_s$. Hence, the input source flux is $F_p = c_s Q_p$. The released passive tracer is set to be unity ($c_s$ = 1) with temperature of the ambient seawater. For the Case 1 (the baseline case), a discharged volume rate is $Q_p = 1.8 \times 10^5\ m^3\ d^{-1}$ and salinity $S$ = 0. The mean surface temperature and salinity of the seawater near the outfall are 23.0 °C and 34.4 psu. In such a situation, the resultant mean density is 1023.48 kg $m^{-3}$, while the freshwater density is 997.55 kg $m^{-3}$. The two alternative scenarios were set as the follows. We reduced discharged volume $Q_p$ from $1.8 \times 10^5\ m^3\ d^{-1}$ to $1.5 \times 10^5\ m^3\ d^{-1}$ in Case 2 (the reduced flux case). And then we increased the sewage density by mixing with the ambient seawater of $0.8 \times 10^5\ m^3\ d^{-1}$ to diminish the surfacing of the buoyant plume in Case 3 (the adjusted buoyancy case). Therefore, the total discharge rate $Q_p$, the density of the mixed effluent $\rho'$, and its salinity $S'$ in Case 3 were modified to $Q_p = 2.6 \times 10^5\ m^3\ d^{-1}$, $\rho'$ = 1005.43 kg $m^{-3}$, and $S'$ = 10.46 psu, respectively. We further modified the input source flux $c_s = (1.8 \times 10^5)/(2.6 \times 10^5) \sim 0.69$ to ensure the total tracer load from the TSTP for Case 3 is equalized to that for Case 1.

## TRACER FLUX ANALYSIS

To quantify the direct impacts of the TSTP on the seaweed farm for the three cases, the tracer flux was calculated with

$$F(\tau) = \int_{A_c} cu_n\,dA_c, \tag{5}$$

where $u_n$ is the velocity perpendicular to the cross-section, and $\tau$ is time. $A_c$ is the cross-sectional area at the corresponding side boundary of the seaweed farm. Because $c$ is non-dimensional concentration, $F$ has the unit of $m^3$ $s^{-1}$. Then we integrate $F$ over a given time period to evaluate cumulative tracer flux $Q$ ($m^3$) for the duration from $\tau =$ 0 to $t$ as follows,

$$Q(t) = \int_0^t F(\tau)\, d\tau, \tag{6}$$

where incoming cumulative tracer fluxes into the farm is defined as positive at the boundaries of the farm. We denote $Q_w$, $Q_n$, $Q_e$, and $Q_s$ as the cumulative flux $Q(t)$ through the western, northern, eastern and southern sections, respectively.

Because there is an obvious different flow patterns between the alongshore and cross-shore directions (U18 [4]), we firstly conduct an effluent flux analysis in the different directions. $Q_w + Q_e$ and $Q_n + Q_s$ are the cumulative tracer fluxes in the alongshore and cross-shore directions. The corresponding temporal variability is shown in **Figure 2a** and **b**. There is an obvious effluent accumulation in the alongshore direction and a reduction in the cross-shore direction. The effluent intrudes into the seaweed farm from the western, northern and eastern sides of the farm, and flow out from the southern transect (U18 [4]). The resultant net accumulation is positive in the alongshore direction and negative in the cross-shore direction. Meanwhile, these temporal changes in the net fluxes for Case 3 and Case 1 are almost coincident, showing that the adjusted buoyancy configuration does not change the sewage transport significantly in both zonal and meridional directions.

The sum of $Q$ at the four vertical cross-sections identifies the net tracer (effluent) flux accumulated in the seaweed farm, *i.e.*, $Q_{farm} = Q_w + Q_n + Q_e + Q_s$. To distinguish $Q_{farm}$ for the three cases, we will respectively denote the net flux as $Q_1$, $Q_2$, and $Q_3$ for $Q_{farm}$ for cases 1, 2, and 3. $\Delta Q_{21}$ and $\Delta Q_{31}$ represent the differences of Case 2 and Case 3 from Case 1. **Figure 2c** denotes the time series of the net tracer budget accumulating in the seaweed farm. The $Q_{farm}$ ($Q_1$, $Q_2$, and $Q_3$) fluctuates periodically at a period of ~14 days, and three peaks appear on Oct. 3, 17, and 21 as summarized in **Table 1**. This periodic behavior indicates that intrusion of the sewage effluent into the seaweed farm occurs mainly at a spring–neap tidal cycle. **Table 1** illustrates that the peaks in $Q_{farm}$ occurred on these three days are $1.84\times10^4$ $m^3$, $3.67\times10^4$ $m^3$ and $5.49\times10^4$ $m^3$ for Case 1, $1.60\times10^4$ $m^3$, $2.78\times10^4$ $m^3$ and $4.15\times10^4$ $m^3$ for Case 2, and $1.85\times10^4$ $m^3$, $3.66\times10^4$ $m^3$ and $5.22\times10^4$ $m^3$ for Case 3, consistent with the accumulations on average during the analysis period. The reduction of the released flux of 16.7% ($1.8 \times 10^5$ $m^3d^{-1}$ → $1.5 \times 10^5$ $m^3d^{-1}$) in Case 2 results in the 25.4% reduction ($2.01 \times 10^4$ $m^3$ → $1.50 \times 10^4$ $m^3$) on average in the accumulation in the farm relative to Case 1. This result indicates that the reduced flux scenario works more than our expectation for the effluent reduction in the farm. By contrast, the difference between Case 3 and Case 1 is subtle, indicating that the density adjustment is not a very effective operation in the present configuration.

## EFFECTS OF MEAN AND TRANSIENT COMPONENTS ON TRACER FLUXES

To examine the possible reason why 16.7% reduction of the input flux results in the 25.4% effluent accumulation decrease in Case 2, we introduce a Reynolds decomposition to the prognostic variables into mean and transient components, in which $c = \bar{c} + c'$ and $u_n = \overline{u_n} + u_n{}'$. Therefore, the time-averaged tracer flux $\overline{cu_n}$ is decomposed as

$$\overline{cu_n} = \bar{c}\,\overline{u_n} + \overline{c'\,\overline{u_n}} + \overline{\bar{c}u_n'} + \overline{c'u_n'} = \bar{c}\,\overline{u_n} + \overline{c'u_n'}, \tag{7}$$

where the overbar denotes the time-averaging operator, and the prime represents the transient component, including the influences from eddies and tides. The first term $\bar{c}\,\overline{u_n}$ represents the linear interaction of the mean tracer concentration $\bar{c}$ and residual currents $\overline{u_n}$, whereas the second term $\overline{c'u_n'}$ stands for the tracer flux associated with the nonlinear interaction of transient currents $u_n'$ with fluctuating tracer concentration $c'$.

The time-averaged tracer flux $\overline{cu_n}$, mean flow component $\bar{c}\,\overline{u_n}$ and transient component $\overline{c'u_n'}$ in the alongshore and cross-shore directions are summarized in **Table 2**. It should be noted that because the tracer flux fluctuates pronouncedly at diurnal and semidiurnal tidal frequency (**Figure 2**), there are slight deviations in the time-averaged results. However, this table is still able to be utilized to conduct a qualitative analysis. The sewage effluent accumulates in the seaweed farm in the alongshore direction and reduces in the cross-shore direction. Compared with Case 1, the effluent reduction occurs in the alongshore direction, whereas the increase appears in the cross-shore direction. In addition, the mean flow component controls the sewage effluent outflow, while the transient component results in incoming tracer flux in the along-shore direction. According to more detailed analysis (not shown here), the difference between two cases indicates that the mean component $\bar{c}\,\overline{u_n}$ enhances effluent accumulation in the farm

particularly at the surface layer, while the transient component $\overline{c'u_n'}$ promotes effluent outflow from the farm in Case 2. Since the western boundary of the seaweed farm is located nearest the outfall, the flux along this section on the net tracer budget is much more prominent than that along eastern section. By contrast, in the cross-shore direction, the decomposed flux results demonstrate a significant predominance of the transient component $\overline{c'u_n'}$ over the mean component $\bar{c}\,\overline{u_n}$. Moreover, compared with Case 1, the transient component $\overline{c'u_n'}$ plays a key role in decreasing the effluent outflux in the farm in Case 2.

## CONCLUSIONS

We utilized the configurations of the validated, quadruple-nested, high-resolution ocean model described in U18 [4] to track the wastewater effluent transport of two more alternative operations at the TSTP in the coastal region and examine its influence on an adjacent seaweed farm. In the reduced flux case, discharged wastewater volume decrease at a rate of 16.7% ($1.8 \times 10^5$ m$^3$ d$^{-1}$ → $1.5 \times 10^5$ m$^3$ d$^{-1}$) contributed to an overall 25.4% reduction of the effluent accumulation in the farm on average ($2.01\times10^4$ m$^3$ → $1.50\times10^4$ m$^3$). To analyze such a nonlinearity, the time-averaged tracer flux was decomposed into the mean and transient flow components. The results illustrated that the mean flow component led to the sewage effluent outflow, while the transient component provoked incoming tracer flux in the along-shore direction. However, as compared to the baseline case, the mean component increased the tracer accumulation in the seaweed farm specially at the surface, while the transient component dominated the tracer reduction in the reduced flux case. The resultant net effects were an overall reduction of tracer accumulation. By contrast, in the cross-shore direction, the transient flow component plays a dominant role in decrease of influx in the reduced flux case. The impact of mean component was much weaker. Concurrently, the transient component was essential to reduction of the effluent outflux compared with the baseline case. For another operation scenario as the adjusted buoyancy case, we modified the wastewater density by mixing with ambient seawater of $8 \times 10^4$ m$^3$ d$^{-1}$ to suppress surfacing of the effluent plume. The adjusted buoyancy scenario did not lead to an obvious effluent accumulation in the farm and the net cumulative tracer fluxes in both zonal and meridional directions, indicating that the density adjustment did not work well to reduce the impacts of the effluent from the TSTP on the farm.

## ACKNOWLEDGMENTS

The present research was financially supported by the City of Kobe and Japan Society for the Promotion of Science (JSPS) Grants-in-Aid for Scientific Research 15KK0207 and 18H03798 at Kobe University. We also appreciate Yota Suzue (CTI Engineering Co., Ltd.) and Taichi Kosako (Port and Airport Research Institute) for their help in the development of the quadruple-nested model.

## REFERENCES

1 Imai, I., M. Yamaguchi and Y. Hori. Eutrophication and occurrences of harmful algal blooms in the Seto Inland Sea, Japan. *Plankt. Benth. Res.* **1(2)**, 71–84, 2006.

2 Terawaki, T., K. Yoshikawa, G. Yoshida, M. Uchimura and K. Iseki. Ecology and restoration techniques for Sargassum Beds in the Seto Inland Sea, Japan. *Mar. Pollut. Bull.*, **47**,198–201, 2003.

3 Tomita, A., Y. Nakura and T. Ishikawa. New direction for environmental water management. *Mar. Pollut. Bull.* **102**, 323–328, 2016.

4 Uchiyama, Y., X. Zhang, Y. Suzue, T. Kosako, Y. Miyazawa, A. Nakayama. Residual effects of treated effluent diversion on a seaweed farm in a tidal strait using a multi-nested high-resolution 3-D circulation-dispersal model. *Mar. Pollut. Bull.* **130**, 40–54, 2018, doi: 10.1016/j.marpolbul.2018.03.007

5 Shchepetkin, A. F. and J. C. McWilliams. The regional ocean modeling system (ROMS): a split-explicit, free-surface, topography-following-coordinate oceanic model. *Ocean Modell.* **9**, 347–404, 2005.

6 Uchiyama, Y., E.Y. Idica, J. C. McWilliams and K. D. Stolzenbach. Wastewater effluent dispersal in Southern California Bays. *Cont. Shelf Res.* **76**, 36–52, 2014.

7 Miyazawa, Y., R. Zhang, X. Guo, H. Tamura, D. Ambe, J. Lee, A. Okuno, H. Yoshinari, T. Setou and K. Komatsu. Water Mass Variability in the Western North Pacific Detected in 15-Year Eddy Resolving Ocean Reanalysis. *J. Oceanogr*. **65**, 737–756, 2009.

8 Mason, E., M. J. Molemake, A. F. Shchepetkin, F. Colas, J. C. McWilliams and P. Sangrà. Procedures for offline grid nesting in regional ocean models. *Ocean Modell*. **35**, 1–15, 2010.

9 Kamidaira, Y., Y. Uchiyama and S. Mitarai. Eddy-induced transport of the Kuroshio warm water around the Ryukyu Islands in the East China Sea. *Cont. Shelf Res*., **143**, 206–218, 2017, doi:10.1016/j.csr.2016.07.004.